Available online at www.sciencedirect.com
SCIENCE DIRECT
Applied Catalysis A: General 309 (2006) 106–114
APPLIED CATALYSIS A: GENERAL
www.elsevier.com/locate/apcata

Liquid phase alkylation of phenol with 1-octene over large pore zeolites

Smita Wagholikar, S. Mayadevi, S. Sivasanker *

National Chemical Laboratory, Pune 411008, Maharashtra, India

Received 14 December 2005; received in revised form 26 April 2006; accepted 27 April 2006
Available online 12 June 2006

Abstract

A comparative study is presented of the liquid phase alkylation of phenol with 1-octene over different zeolite catalysts: H-beta (BEA(15)), H-mordenite (MOR(11)) and H-USY (FAU(15)). A wide spectrum of monoalkylated products, identified as isomers of phenyl octyl ether (*O*-alkylate) and octyl phenol (*C*-alkylate), was formed in the reaction. The reaction was studied in detail over BEA(15), such studies included the influence of process variables such as temperature, reactant mole ratio, catalyst amount and alkali metal (K) poisoning on its performance in the alkylation reaction. A kinetic analysis of the reaction over BEA(15) was also carried out assuming a second order parallel reaction mechanism. The activity of the different catalysts for the reaction followed the order: BEA(15) > FAU(15) > MOR(11). The poisoning of BEA(15) with potassium resulted in a decrease in the catalyst activity concomitant with a decrease in the number of strong acid centres in the catalyst.

Keywords: Alkylation; Phenol; 1-Octene; Alkyl phenols; Zeolites

1. Introduction

Long-chain ($>C_8$) alkyl phenols are used in the industry in the manufacture of surfactants, as antioxidants and as additives in lubricants and plastics. These are typically manufactured by the alkylation of phenol with the corresponding long-chain olefins or alcohols over acid catalysts such as BF_3 and ion-exchange resins. Zeolites are strongly acidic solids and their use in alkylation reactions has many benefits like ease of separation of the product, avoidance of corrosion problems, negligible waste and byproduct formation and reusability due to greater thermal stability. The alkylation of phenol with olefins and alcohols has been studied in both the liquid and the vapour phase by different groups using zeolites [1–6], SAPO-11 [7] and mesoporous materials [8,9] as catalysts. A high yield of *p*-tertiary butyl phenol (*p*-TBP) has been reported in the vapour phase *tert*-butylation of phenol over H-beta (BEA) at 418 K at low reactant molar ratios [5,6]. It is reported that medium acid sites on the zeolite are advantageous in producing *p*-TBP, that strong acid sites are helpful for the formation of 2,4-ditertiary butyl phenol (2,4-DTBP) and that weak acid sites are responsible for the formation of *o*-TBP. In SAPO-11, the reaction is reported to take place inside the catalyst pores. Poisoning of the acid sites by ammonia and quinoline reduced the activity, revealing the roles played by weak and strong acid sites in the reaction [7]. Sakthivel et al. have reported that phenol conversion increases with a decrease in the phenol: *t*-BuOH ratio over H-AlMCM-41 [8]. When *tert*-butylation was carried out over mesoporous H-FeMCM-41, *p*-TBP was obtained as the major product with high selectivity [9]. The alkylation of phenol with long chain olefins or alcohols yielded a broad spectrum of products that included products from octene isomerization. Young [10] reported that the product distribution varied depending on the catalyst pore size. Preferential *para*-substitution occurred, leading to selective formation of *p*-octyl phenol when large pore zeolites were used as catalysts [11]. The less bulky 2-octyl phenol was equally favoured over REY, MOR and MTW. Sonawane et al. [12–14] observed both ring alkylation (*C*-alkylation) and ether formation (*O*-alkylation) in the homogeneous liquid phase alkylation of phenol using 1- and 2-octenes in the absence of solvent at room temperature over BF_3-etherate catalyst. The *O*-alkylate was found to contain isomeric 2-, 3- and 4-octyl phenyl ethers. The terminal olefin was more reactive in the reaction as compared to 2-octene. The reaction initially favoured the formation of the 2-isomer, while 1-octyl phenyl ether was totally absent. Hu et al. have investigated the use of heteropolyacids supported on SiO_2, alumina and diatomaceous

* Corresponding author. Fax: +91 20 2589 3761/3260.
E-mail address: s.sivasanker@ncl.res.in (S. Sivasanker).

0926-860X/$ – see front matter © 2006 Elsevier B.V. All rights reserved.
doi:10.1016/j.apcata.2006.04.041

earth in the alkylation of phenol with 1-octene and nonene [15]. The authors have reported the formation of mainly the alkyl phenols predominantly of the *p*-form over these catalysts. Similarly, Halligudi and co-workers have also reported the formation of mainly the alkyl phenols (mono and dialkyl) during the alkylation of phenol with 1-octene, 1-decene and 1-dodecene over WO_x/ZrO_2 mixed oxide catalysts [16].

In this paper we present a comparative study of the liquid phase alkylation of phenol with 1-octene over different zeolite catalysts, H-beta (BEA(15)), H-mordenite (MOR(11)) and H-USY (FAU(15)), the numbers in parentheses referring to the Si/Al ratio of the zeolites. The influence of process variables such as temperature, reactant mole ratio, catalyst amount and alkali metal poisoning on the reaction has been investigated over BEA(15).

2. Experimental

2.1. Catalysts

The H-forms of zeolites beta (BEA(15)), Y (FAU(15)) and mordenite (MOR(11)) were obtained from PQ Corp., USA. The zeolites were calcined at 723 K for 4 h and then stored in sealed bottles. XRD patterns of the zeolites matched well with their standard patterns. A comparison of the physical characteristics of the catalysts is presented in Table 1.

Poisoning of beta with potassium was carried out by treating the zeolite (NH_4-BEA) with different quantities of a 0.03 M solution of K_2CO_3 at 353 K for 1 h. The zeolite was then filtered, dried (373 K, 12 h) and calcined (773 K, 6 h). The alkali metal content was estimated by atomic absorption spectroscopy. The samples contained 0.1–0.4 mmol of alkali metal per gram (Table 2).

2.2. Catalyst characterization

The catalysts (fresh/poisoned) were characterized for their crystallinity, surface area and acidity by X-ray diffraction (XRD), N_2 adsorption, and temperature programmed desorption (TPD) of ammonia, respectively. Surface areas of the samples were obtained by both the BET and point-B methods [17]. Acidity of the zeolites was characterized by the TPD of NH_3 (Micromeritics, Autochem 2910). The standard procedure for TPD measurements involved the activation of the zeolite in flowing He at 873 K (3 h), cooling to 298 K and adsorbing NH_3 from a stream of He–NH_3 (10%), removing the physically adsorbed NH_3 by desorbing in He at 373 K for 1 h and finally carrying out the TPD experiment by raising the temperature of the catalyst in a programmed manner (10 K min^{-1}). The TPD curves were deconvoluted into two peaks and the areas under the peaks were converted into milliequivalents (meq) of NH_3 per gram of catalyst based on injection of known volumes of the He–NH_3 mixture at similar conditions.

Table 1
Physical characteristics of zeolite catalysts

Sample name[a]	(Al/Si + Al) ratio	Surface area (m^2/g)			Acidity (meq/g)		
		S_{BET}	S_B[b]	External[c]	Total	Weak	Strong
BEA(15)	0.0625	656	681	166	1.22	0.55	0.67
MOR(11)	0.0833	562	593	52	1.87	1.05	0.82
FAU(15)	0.0625	697	728	93	0.58	0.14	0.44

[a] The number in the parentheses is the Si/Al ratio of the sample.
[b] Surface areas have been calculated from V_m values obtained by the point-B method.
[c] Calculated by the t-plot method.

Table 2
Acidity of BEA samples (fresh and poisoned) from TPD of NH_3

K (mmol/g)	Acidity (meq/g)		
	Total	Weak	Strong
Nil	1.21	0.55	0.66
0.1	1.02	0.46	0.57
0.3	0.88	0.49	0.39
0.4	0.45	0.50	0.22

2.3. Alkylation of phenol with 1-octene

The reactions were carried out in a two-necked RB flask (25 cm^3) using equimolar amounts of phenol and 1-octene (10 mmol each) and 0.2 g of freshly calcined catalyst, in a N_2 atmosphere. Aliquots of the reaction were collected at different time intervals and analyzed by gas chromatography (Varian Star 3400 C_X; capillary column: CP Sil 5CB, 30 m and i.d. 0.05 mm). The reaction products were identified by GC–MS and GC–IR. The standard compounds required for the GC analysis were synthesized in the laboratory following established organic synthesis methods.

3. Results and discussion

3.1. Physicochemical properties of the catalysts

The results of the physicochemical investigations are presented in Table 1. As the BET equation is not expected to be applicable in the case of microporous materials, monolayer volumes were also calculated from the adsorption isotherms by the point-B method typically used for Type-II adsorption isotherms as is usually observed in the case of micro and mesoporous materials [17]. The surface area values obtained by the point-B method were slightly larger than those obtained by the BET method, the differences being about 3.8% for BEA(15), 5.5% for MOR(11) and 4.4% for FAU(15). The external surface areas of the samples were obtained by the *t*-plot method. The BEA sample had a much larger external surface area (166 m^2/g) than the MOR and FAU samples (52 and 93 m^2/g, respectively).

The TPD (of adsorbed NH_3) profiles essentially consisted of two unresolved peaks for all the samples. These were deconvoluted into two distinct peaks with peak maxima around 450 (±20) K for first peak and 650 (±50) K for the second peak. It was assumed that the two peaks represent NH_3 adsorbed from weak and strong acid sites. Based on this assumption and the amount of NH_3 desorbed, as obtained from

the area under the corresponding peaks, strong and weak acidity (in meq/g) have been calculated and reported in Table 1. It is seen from the table that MOR(11) is more acidic than the other two zeolite samples. It is also observed that the strong acidity (expected to arise from the framework Al-ions) is nearly proportional to the Al-content (Al/Si + Al; Table 1) for BEA and MOR. However, the amount of strong acidity is found to be slightly lower in Y. The number of acid sites in a given zeolite is expected to be proportional to its Al content only if all the Al-ions are present in the framework. However, such a one to one correlation of acidity with Al content is not always possible, especially in the case of commercial zeolites, due to the presence of varying amounts of extra-framework Al-ions in the samples. The influence of K-loading on the acidity of BEA(15) is presented in Table 2. The addition of K decreases primarily the strong acid sites in the sample without having much effect on the weak acid centers. The decease in strong acidity is found to be proportional to the K-loading suggesting that each K atom destroys one strong acid site.

3.2. Alkylation of phenol with 1-octene

The alkylation of phenol with 1-octene over the zeolite catalysts resulted mainly in the formation of the monoalkylated products. In the absence of a catalyst, the reaction did not proceed to any appreciable extent at the end of 6 h even at 383 K. The reaction between phenol and 1-octene over the catalysts produced mainly oxygen alkylated (*O*-alkylated) and carbon alkylated (*C*-alkylated) products. These appear to be formed in parallel and constitute isomeric (2-, 3- and 4-) octyl phenyl ethers (*O*-alkylates) and octyl phenols (*C*-alkylates) (Fig. 1).

3.2.1. Influence of reaction time

The plots of the changes in conversion, product profile and the *O*-alkylate to *C*-alkylate ratio with time obtained at 373 K over BEA(15) are presented in Fig. 2(a–c). The major products formed during the reaction are phenyl octyl ether (*O*-alkylate), and the *ortho*- and *para*-substituted octyl phenols mentioned independently as the *o*- and *p*-products, and together as the *C*-alkylate. At 373 K, the concentration of *O*-alkylate is larger than the concentration of either the *o*- or the *p*-product. However, the *C*-alkylate (*o*- + *p*-) formation is always more than that of the *O*-alkylate, suggesting a greater activity of the catalyst for *C*-alkylation than for *O*-alkylation. The greater *C*-alkylation may also be due to the fact that at least three carbon positions (*o*- and *p*-) in the ring are available for *C*-alkylation, whereas only one oxygen atom is available for *O*-alkylation. The selectivity ratio (*O*-alkylate/*C*-alkylate) decreases with increase in time. Based on high temperature studies, earlier workers have suggested that the ether (*O*-alkylate) is formed even over weak acid centers, while *C*-alkylation requires stronger acid sites [6,8,12]. Also, an increase in *O*-/*C*-alkylate ratio with time on stream in the temperature range of 473–673 K for both liquid and vapour-phase experiments has been reported in the alkylation of phenol with methanol, which was attributed to catalyst deactivation [8,12]. Our observation on the changes in *O*-/*C*-ratio with run duration is different (Fig. 2b). One reason for the difference could be the different alkylating agents used in the experiments, methanol by earlier workers and 1-octene by us. However, an explanation for the observed differences over the two alkylation agents is not possible without an understanding of the nature and strength of the adsorbed species for the two reactants and the required intermediates for the two reactions. As we found that the reaction of 2-octyl phenyl ether over BEA at 373 K did not produce any isomerization products even at the end of 6 h of reaction, the isomerization of the ether into alkyl phenols is not a likely reason for our observations. Though the exact reason for the observed decrease in the *O*-/*C*-ratio with run duration is not clear, it may be also be due to greater deactivation of the sites responsible for *O*-alkylation.

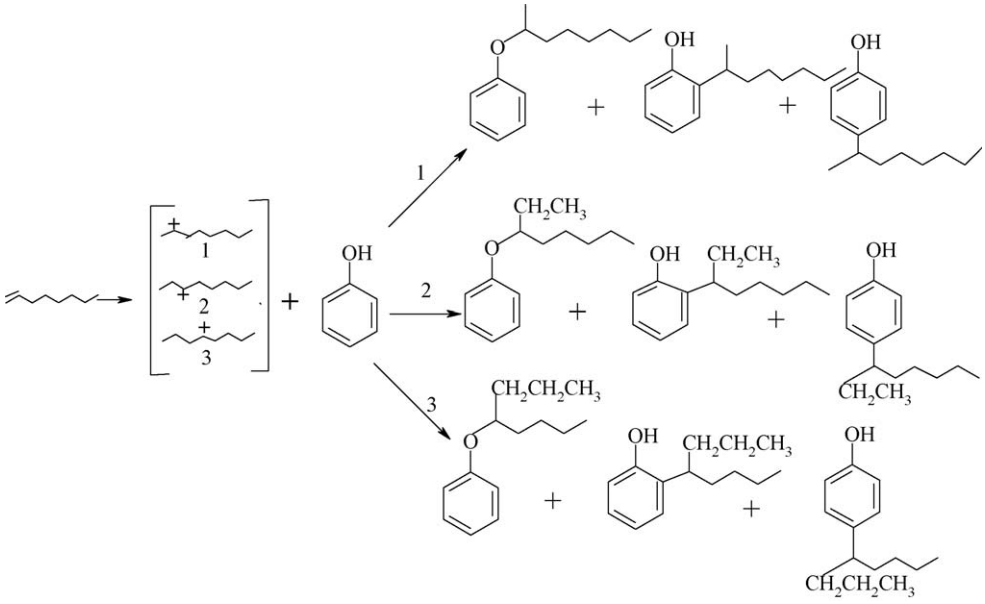

Fig. 1. The reactions in the alkylation of phenol with 1-octene.

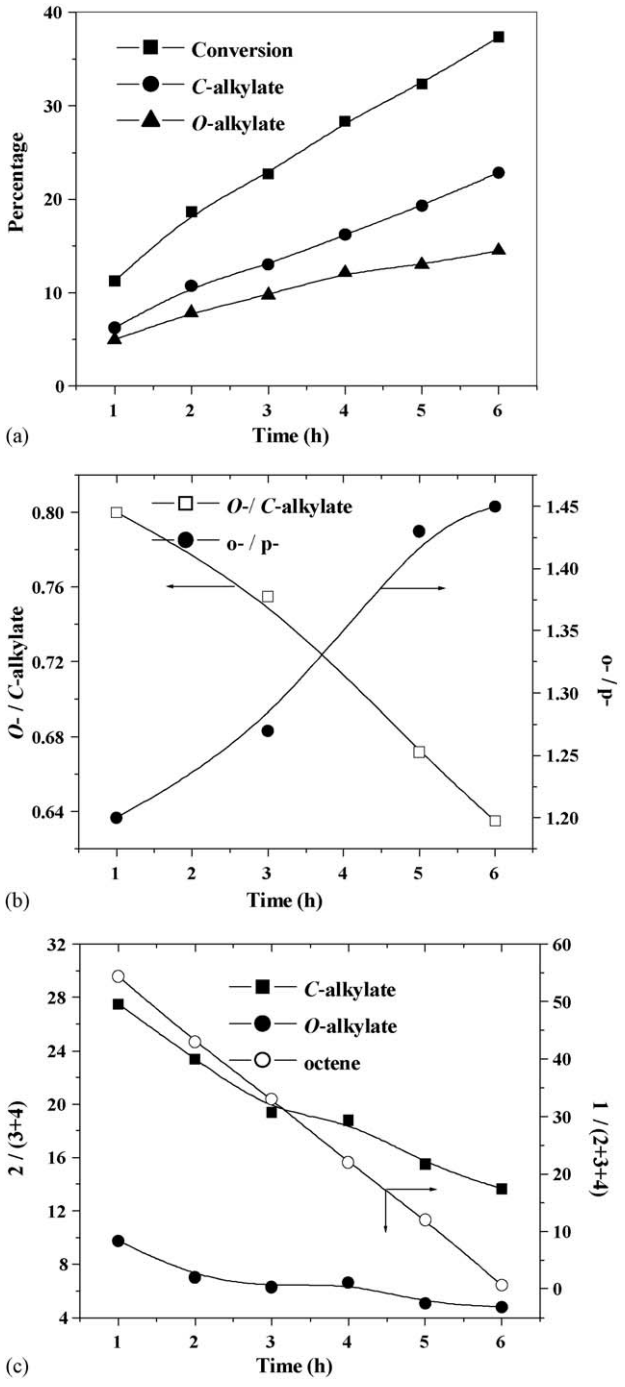

Fig. 2. Influence of duration of run on (a) conversion and yields of *O*- and *C*-alkylate, (b) *O*-/*C*-alkylate and *o*-/*p*-ratios and (c) ratios of skeletal isomers in *O*- and *C*-alkylate and ratios of olefins (*catalyst*: BEA, 0.2 g; *temperature*: 373 K; phenol:1-octene (mole) = 1).

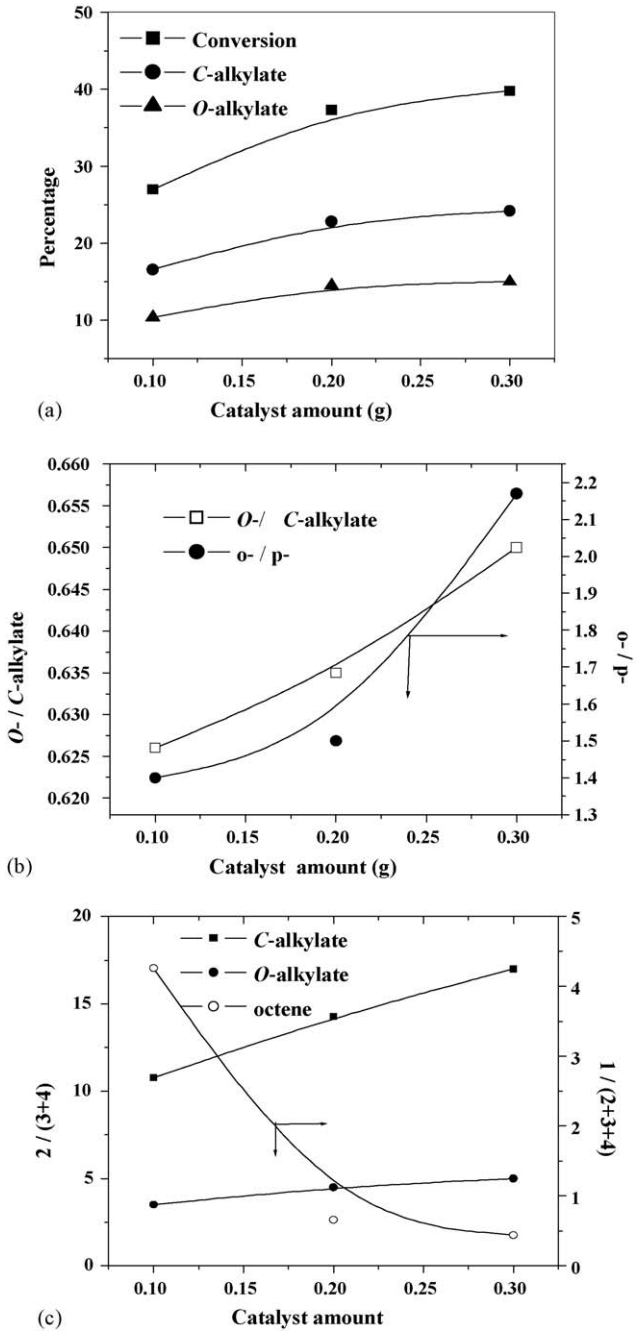

Fig. 3. Influence of catalyst amount on (a) conversion and yield of *C*-and *O*-alkylates, (b) *O*-/*C*-alkylate and *o*-/*p*-ratios and (c) ratios of skeletal isomers in *O*- and *C*-alkylate and ratios of olefins (*catalyst*: BEA, 0.2 g; *temperature*: 373 K; phenol:1-octene (mole) = 1:1; *duration of run*: 6 h).

Three isomeric *O*- and *C*-alkylates corresponding to the positions of the phenoxy or phenyl group in the octane chain at 2-, 3- and 4-positions are found in the product mixture. The 1-isomer is not formed due to the poor stability of the 1-carbenium ion. At equilibrium, one would expect approximately equal amounts of the three isomers and a 2-/(3- + 4-) ratio of about 0.5. However, one can notice (Fig. 2c) that the experimentally observed ratio is much higher. The deviation from equilibrium is much larger for the *C*-alkylate than for the *O*-alkylate. With duration of run, the (2-/(3- + 4-)) ratio decreases for both the *C*- and *O*-alkylates. Two different equilibrium steps can exist in the overall reaction: one for the equilibration of the olefin (octene) and another for the equilibration of the alkyl phenols/ethers [8]. At the low temperature used in this study (373 K), the latter equilibration reaction is expected to be much slower than olefin equilibration. The large amount of the 2-isomer observed in the products is due the greater reactivity of the terminal olefin compared to the

Table 3
Effect of mole ratio of phenol and 1-octene on conversion and product yield

Phenol:1-octene (mole)	Conversion of phenol (%)	Product yield (%)			*O*-/*C*-alkylate	*o*-/*p*-alkylate	2/(3 + 4)	
		O-alkylate	*Ortho*-alkylate	*Para*-alkylate			*O*-	*C*-
1:0.5	11.3	4.9	3.9	2.6	0.72	1.5	5.4	23.6
1:1	37.3	14.5	13.5	9.3	0.64	1.5	4.8	13.7
1:2	42.0	9.0	22.0	11.0	0.2	2.0	2.1	8.2

Conditions: temperature, 373 K; catalyst, BEA(15), 0.2 g; reaction time, 6 h; atmosphere, N_2.

reactivities of the internal olefins [9–11] and the non-attainment of olefin equilibrium. The larger values of the (2-/(3- + 4-)) ratio for *C*-alkylation than for *O*-alkylation is probably due to many causes, like differences in the reactivity of the olefins, different spatial and steric requirements for the different transition states inside the pores, acidity distribution and the difference in the relative contribution of the external and internal areas to the two reactions.

3.2.2. Influence of catalyst quantity and mole ratio of the reactants

The influence of catalyst quantity (0.1–0.3 g) on the reaction at 373 K over BEA(15) is presented in Fig. 3. There is a marginal increase in conversion and product formation on increasing the catalyst quantity from 0.1 to 0.3 g, the increase being less after 0.2 g. A catalyst quantity of 0.2 g was used in all the subsequent experiments. Both *O*-/*C*-ratio and *o*-/*p*-ratio increase with increase in catalyst amount (Fig. 3b). Again, the (2-/(3- + 4-)) isomer ratio also increases with increasing catalyst amount (Fig. 3c). This suggests that the reactant 1-octene is more rapidly converted into the alkylation products than into isomeric octenes when there is more catalyst. The 1-octene content in the product decreases rapidly on increasing catalyst loading, due to the greater reactivity of the 1-octene for the alkylation reaction and its isomerization into the internal olefins.

The influence of the phenol- to 1-octene mole ratio on the reaction is presented in Table 3. Phenol conversion increases with increasing amount of 1-octene (higher octene: phenol ratio). The *O*-alkylate content of the product is largest when the mole ratio of the two reactants is 1. The *C*-alkylate formation increases with increasing octene concentration causing the *O*-/*C*-alkylate ratio to decrease. The *o*-/*p*-alkylate ratio is apparently not significantly affected by changes in the mole ratio (studied between 0.5 and 2) and is in the range 1.5–2 for the concentrations investigated. The (2-/3- + 4-) ratios of both the *C*- and the *O*-alkylates decrease with increasing octene content. This could be due to greater competition from the isomerization reaction at higher octene content in the reaction mixture. Also, as already reported, the (2-/(3- + 4-)) ratio is larger for the *C*-alkylate than for the *O*-alkylate.

3.2.3. Influence of reaction temperature

The influences of reaction temperature on conversion and product ratios (recorded at a constant run time of 6h) are presented in Fig. 4(a–c). As expected, the conversion of phenol increases with increase in the alkylation temperature (Fig. 4(a)). Also, both *O*-/*C*- and *o*-/*p*-ratios increase with temperature (Fig. 4b). Apparently, the formations of the *O*-alkylate and the *o*-isomer in the *C*-alkylate are more favoured than the formations of the other products at higher temperatures. The (2-/(3- + 4-)) isomer ratio decreases for both the alkylation products (Fig. 4c). Similarly, the 1-octene content also decreases with increasing temperature suggesting more rapid isomerization of 1-octene at higher temperatures. The apparent activation energies calculated based on the rate constants are presented in a later section.

3.2.4. Influence of poisoning of catalyst with potassium

The effect of acidity on the two major reactions was investigated by systematic poisoning of BEA with small amounts of potassium. The acidity of the poisoned catalysts calculated from TPD of NH_3 is presented in Table 2 and the TPD profiles are presented in Fig. 5. The influence of poisoning BEA(15) with potassium on conversion and selectivity for different products is presented in Fig. 6(a–c), respectively. The figures show that the catalyst activity is significantly decreased by potassium loading; it decreases from 37% to 9% with the addition of 0.4 mmol of K per g of BEA. The *O*-/*C*-alkylate ratio is not significantly affected by K-loading while the *o*-/*p*-ratio shows a distinct increase. TPD plots in Fig. 5 show that the addition of K leads to a reduction in acid sites. Table 2 shows that the strong acidity of the catalysts decreases preferentially (without much change in the amount of weak acid sites) with an increase in the alkali metal content. This decrease in strong acidity is found to be nearly quantitative, approximately the same amount (meq per g) of strong acidity being destroyed by an equivalent amount of K (Table 2).

3.2.5. Influence of zeolite type

A comparative study was carried out of the activities of the three large pore zeolites: BEA(15), MOR(11) and FAU(15) (H-USY) in the alkylation of phenol with 1-octene. The results of the reaction carried out at 373 K are presented in Table 4. The ratio of skeletal isomers is also presented in the table.

The data collected at different run durations for MOR(11) and FAU(15) (H-USY) are presented in Figs. 7 and 8, respectively. The data of BEA was presented in Fig. 2. The relative activity of the zeolites for the reaction, in terms of phenol conversion (at 6 h; Table 4) is in the order: BEA(15) > FAU(15) > MOR(11). MOR(11) has the largest amount of acid sites, both strong and weak (Table 1). In spite of this, it has the least activity for phenol alkylation, among the three zeolites. The lower activity of MOR is probably due to its 2-dimensional pore structure and the absence of large pore

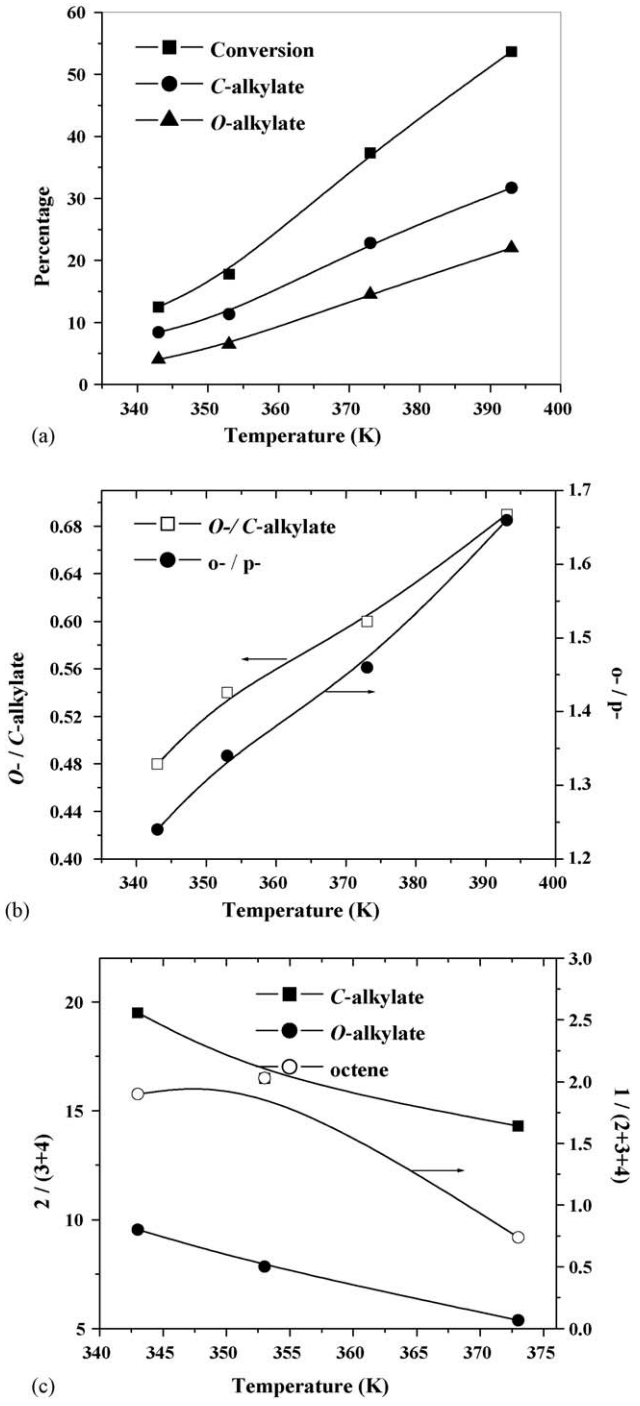

Fig. 4. Influence of temperature of reaction on (a) conversion and yields of *O*- and *C*-alkylate, (b) *O*-/*C*-alkylate and *o*-/*p*-ratios and (c) ratios of skeletal isomers in *O*- and *C*-alkylate and ratios of olefins (*catalyst*: BEA, 0.2 g; phenol:1-octene (mole) = 1; *duration of run*: 6 h).

intersections that can accommodate the large reaction transition state. Conversion increases rather rapidly on both BEA and MOR with run duration (Figs. 2 and 7), but in the case of FAU, the increase with time is only marginal (Fig. 8). It is likely that polymeric products (large molecules) are rapidly formed inside the large α-cages in the FAU (H-USY) and poison the strong acid sites. BEA and MOR favour *C*-alkylate formation, and FAU favours *O*-alkylate formation; the *O*-/*C*-ratios obtained (at

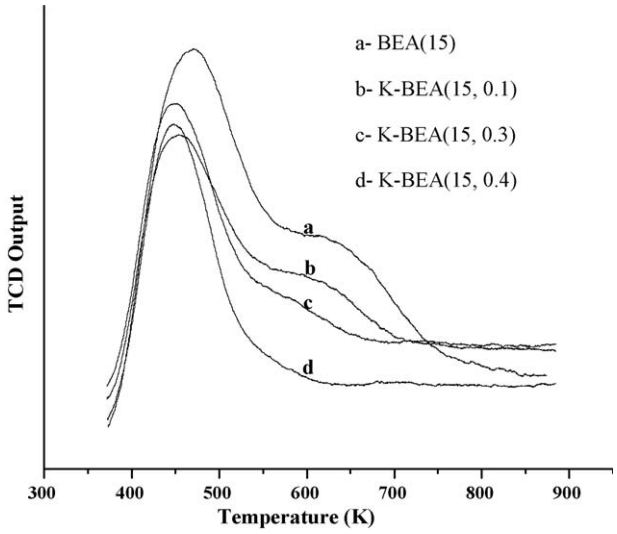

Fig. 5. TPD profiles of ammonia of fresh and potassium poisoned BEA(15) samples (see Table 2).

6 h) over BEA, MOR and FAU are, respectively, 0.6, 0.3 and 1.5. Examining the trend in the *O*-/*C*-ratio, one finds that it increases with time over MOR and FAU, but decreases in the case of BEA.

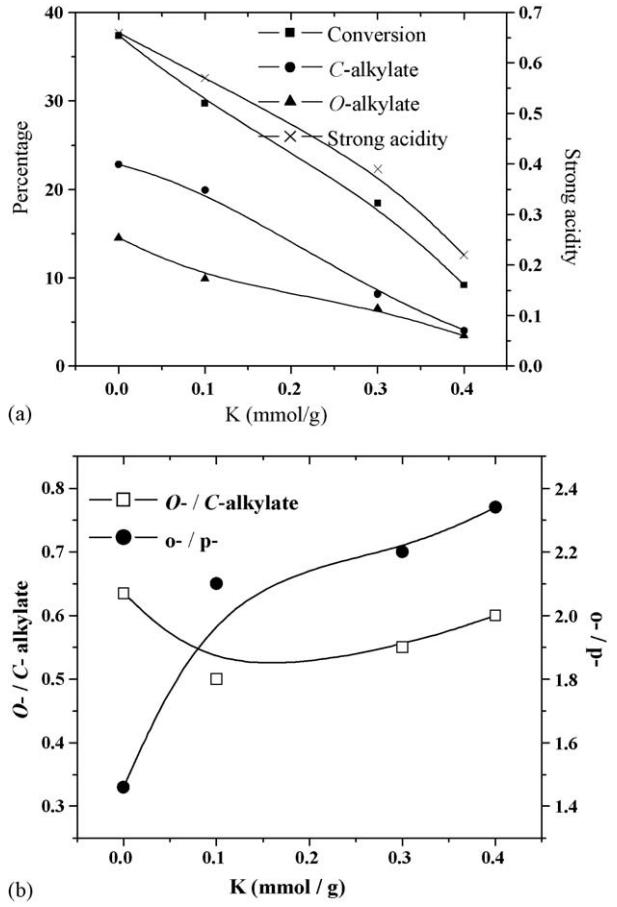

Fig. 6. Influence of K-loading on (a) strong acidity, conversion and yields of *O*- and *C*-alkylate and (b) *O*-/*C*-alkylate and *o*-/*p*-ratios (*catalyst*: BEA, 0.2 g; *temperature*: 373 K; phenol:1-octene (mole) = 1; duration of run: 6 h).

Table 4
Effect of zeolite type on conversion and product yield in the alkylation of phenol with 1-octene

Zeolite	Conversion of phenol (%)	Product yield (%)			*O*-/*C*-alkylate	*o*-/*p*-	2/(3 + 4)	
		O-alkylate	*Ortho*-alkylate	*Para*-alkylate			*O*-	*C*-
BEA(15)	37.3	14.5	13.5	9.3	0.64	1.45	4.8	13.6
FAU(15)	30.5	18.2	8.0	4.2	1.49	1.90	5.8	6.4
MOR(11)	10.3	2.4	4.4	3.6	0.30	1.22	6.7	17.6

Conditions: temperature, 373 K; catalyst quantity, 0.2 g; reaction time, 6 h; atmosphere, N_2.

All the three catalysts favour the *o*-isomer formation; the *o*-/*p*-ratios (at 6 h) over BEA, MOR and FAU are, respectively, 1.5, 1.2 and 1.9. The lowest *o*-/*p*-ratio observed for MOR suggests that product or transition state shape selectivity may be operating in the catalyst. In all the three zeolites, the *o*-isomer is formed preferentially due to kinetic effects. The (2-/(3- + 4-)) ratios for the *C*-alkylate are larger (in the case of all the three zeolites) than for the *O*-alkylate (Table 4).

3.3. Kinetic Analysis

The alkylation of phenol with 1-octene is rather complex, involving a number of possible reactions. The major reaction products are represented in Fig. 9a. The product analysis for this reaction, when phenol and octene are taken in the molar ratio 1:1, predominantly showed the formation of *O*-alkylation (ether) and *C*-alkylation products (*o*-alkyl phenol and *p*-alkyl phenol). For analytical simplicity, the isomerization of octene was ignored and the overall reaction was considered as a set of parallel reactions resulting in the formation of ether and alkyl phenols. This is justified because the products from octene isomers constituted only a small amount of the products of the overall reaction. This is schematically represented in Fig. 9b as a set of second order reactions in parallel. The general equation for a second order irreversible reaction with equi-molar reactants is given by:

$$\frac{X_A}{(1 - X_A)} = C_{A_0} kt$$

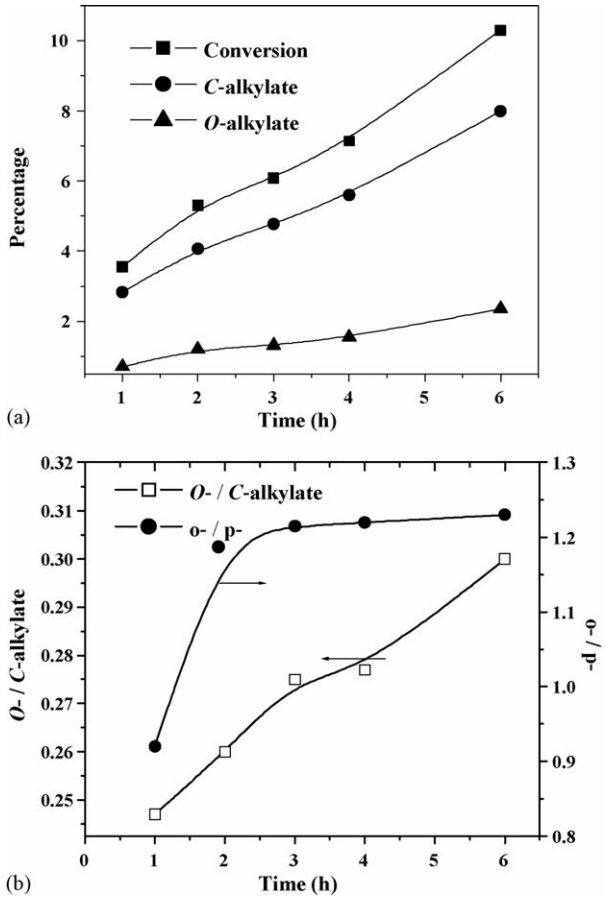

Fig. 7. Influence of duration of run on (a) conversion and yields of *O*- and *C*-alkylate and (b) *O*-/*C*-alkylate and *o*-/*p*-ratios (catalyst: MOR(11), 0.2 g; temperature: 373 K; phenol: 1-octene (mole)∷1).

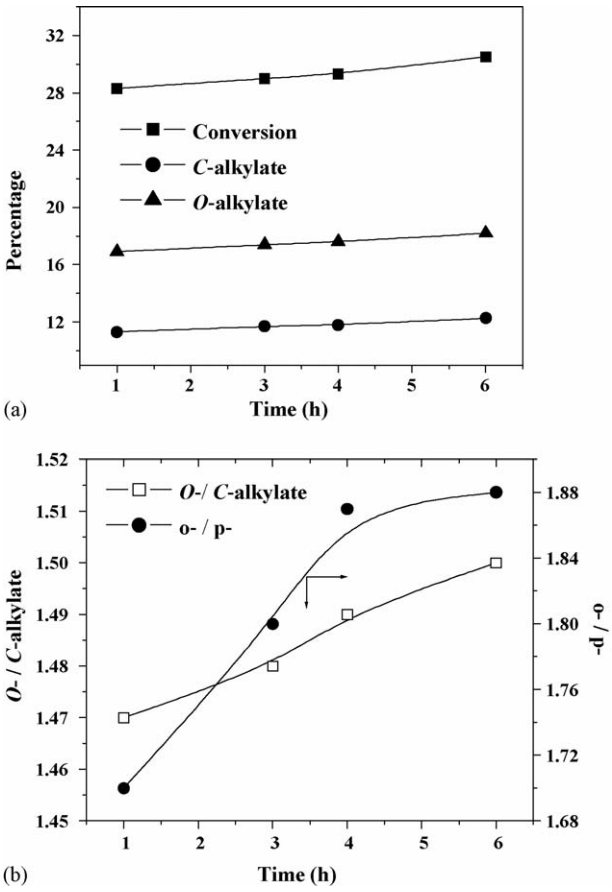

Fig. 8. Influence of duration of run on (a) conversion and yields of *O*- and *C*-alkylate and (b) *O*-/*C*-alkylate and *o*-/*p*-ratios (*catalyst*: FAU(15) (H-USY), 0.2 g; *temperature*: 373 K; phenol:1-octene (mole)∷1).

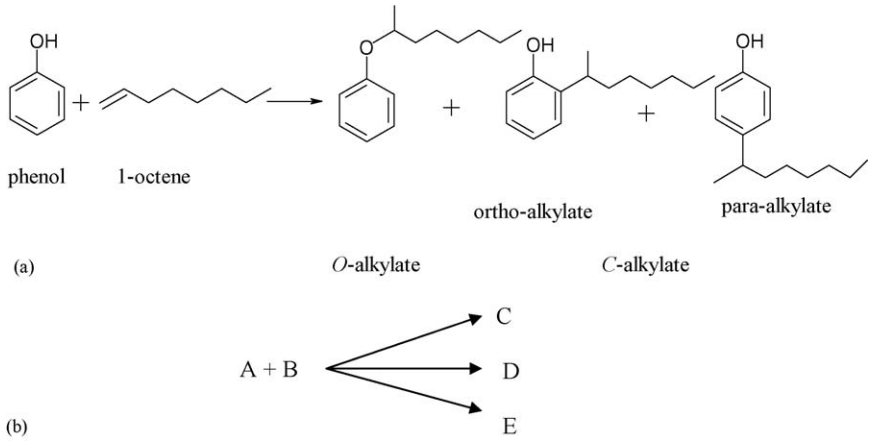

Fig. 9. (a) Major products in the alkylation of phenol with 1-octene. (b) Schematic representation of the simplified reaction path.

Here X_A is the conversion of reactant A, which is the same as that of reactant B, C_{A_0} the initial number of moles of reactant A or reactant B, t the reaction time and k is the second order reaction rate constant. The rate constants of the reactions at different reaction temperatures were calculated using the above expression and the temperature dependence of the rate constant was evaluated using the Arrhenius expression:

$$k = k_0\, e^{(-E/RT)}$$

In the above expression, k_0 is the frequency factor, E the activation energy, R the universal gas constant and T is the reaction temperature.

3.3.1. Temperature dependence of the reaction rate constants

Phenol alkylation reaction has been considered as a set of second order reactions in parallel forming *O*-, *ortho*- and *para*-products. The *o*- and *p*-products together were considered as the *C*-alkylates. The rate constants for the overall reaction, as well as the individual reactions as a function of the reaction temperature, are presented in Fig. 10 as Arrhenius plots. The rate constants for the overall reaction as well as the individual reactions increase with increasing temperature. The rate constant for the *C*-alkylated products ($k_{ortho\text{-alkylate}} + k_{para\text{-alkylate}}$) is higher than that for the *O*-alkylated product in the entire temperature range under study. The activation energy values (calculated from Fig. 10) for the overall reaction and the *O*- and *C*-alkylation reactions are presented in Table 5. The equations for the rate constants are also given in the table. The table shows that activation energies for the two major reactions are similar, the value for *O*-alkylation being marginally larger.

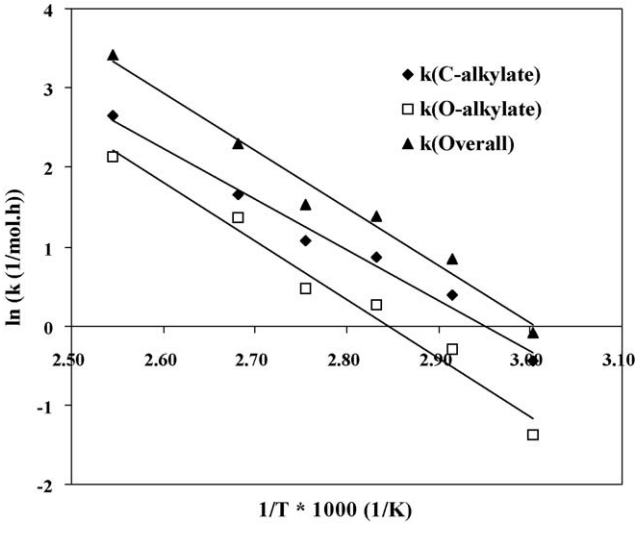

Fig. 10. Arrhenius plots for product formation in the alkylation of phenol with 1-octene (*catalyst*: BEA, 0.2 g; phenol:1-octene (mole)∷1).

3.3.2. Influence of K-poisoning on the reaction rate constants

The reaction rates for both *O*- and *C*-alkylation are affected by poisoning of BEA(15) with small amounts of potassium as can be seen from Fig. 11a. The rate constants calculated for total conversion and for *O*- and *C*-alkylate formation show a decrease as the potassium loading increases. A noticeable decrease in the *k*-value for *O*-alkylation is observed even at the lowest concentration of K (0.1 mmol/g), while the *C*-alkylation reaction is less affected. The catalyst activity is found to decrease rapidly at higher K-loadings. A plot of the *k*-values as a function of the number of strong acid centers in the K-poisoned samples is presented in Fig. 11(b). Both the *O*- and *C*-alkylation activities are directly related to the strong acidity. Already, it was reported (Table 2) that K-loading causes a preferential and quantitative decrease in strong acid centres.

Table 5
Activation energy and the equations for temperature variation of rate constants for phenol alkylation with 1-octene

Reaction	Activation energy (kcal/mole)	Equation for rate constant
Formation of *O*-alkylate	14.60	$k_{O\text{-alkyl}} = 1.0E{+}09\ e^{(-14.60/RT)}$
Formation of *C*-alkylate	12.64	$k_{C\text{-alkyl}} = 2.0E{+}08\ e^{(-12.64/RT)}$
Overall reaction	14.53	$k_{overall} = 3.0E{+}09\ e^{(-14.34/RT)}$

Conditions: catalyst, BEA, 0.2 g; phenol:1-octene (mole)∷1.

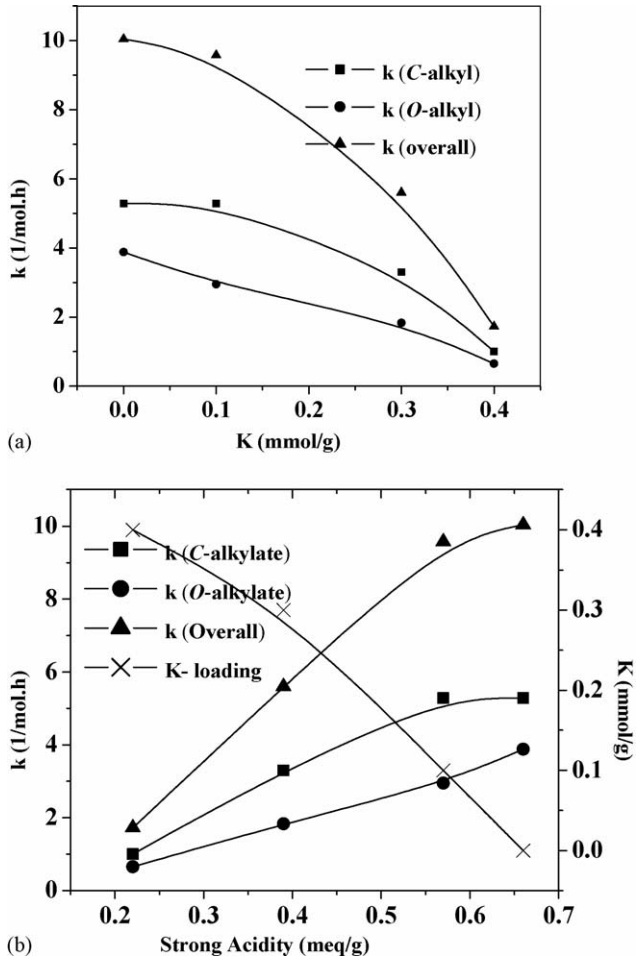

Fig. 11. (a) Effect of poisoning of BEA-15 (with K), and (b) influence of acidity and K-content on the rate constants of different reactions in alkylation of phenol with 1-octene (*temperature*: 373 K; *catalyst weight*: 0.2 g; phenol: 0.01 mol; phenol:1-octene = 1).

4. Conclusions

The liquid phase alkylation of phenol with 1-octene over BEA(15), MOR(11) and FAU(15) produced mainly mono-alkylates and there was no reaction in the absence of catalyst. The major products formed were phenyl octyl ether (*O*-alkylate) and *ortho* and *para* substituted octyl phenols (*C*-alkylates). The reaction favors the formation of *C*-alkylates over *O*-alkylates, and the formation of 2-octyl phenol and 2-phenyl ether among the different chain isomers (2-, 3- and 4-alkylates). Poisoning of the catalyst with potassium resulted in a decrease in the number of strong acid sites and in catalyst activity.

Among the different zeolite catalysts tested for the reaction, MOR(11) was the most acidic (more strong and weak acid sites). In spite of this, it had the lowest activity for phenol alkylation due to its two-dimensional structure and the absence of large pore intersections to accommodate the large transition state. The activity of the catalysts for the alkylation reaction followed the order: BEA(15) > FAU(15) > MOR(11).

A kinetic analysis of phenol alkylation reaction was carried out considering it as a set of second order parallel reactions resulting in the formation of ether (*O*-alkylate) and *ortho*- and *para*-alkyl phenols (*C*-alkylates). The activation energy for *O*-alkylate formation was marginally larger than for *C*-alkylate formation resulting in larger *O*-/*C*-ratios at higher temperatures. However, the rate constant for *C*-alkylate formation was higher than for *O*-alkylate formation in the temperature range investigated (343–393 K).

References

[1] J. Xu, A. Yan, Q. Xu, React. Kinet. Catal. Lett. 62 (1997) 71.
[2] S. Balsaam, P. Beltrame, P.L. Beltrame, P. Carniti, L. Forni, G. Zuretti, Appl. Catal. 13 (1984) 161.
[3] R. Pierantozzi, A.F. Nordquist, Appl. Catal. 21 (1986) 263.
[4] K. Zhang, C. Huang, H. Zhang, S. Xiang, S. Lui, D. Xu, H. Li, Appl. Catal. A: Gen. 207 (2001) 183.
[5] K. Zhang, C. Huang, H. Zhang, S. Xiang, S. Lui, D. Xu, H. Li, Appl. Catal. A: Gen. 166 (1998) 89.
[6] A.V. Krishnan, K. Ojha, N.C. Pradhan, Org. Proc. Res. Dev. 6 (2002) 132.
[7] S. Subramaniam, A. Mitra, C.V.V. Satyanarayana, D.K. Chakrabarty, Appl. Catal. A: Gen. 159 (1997) 229.
[8] A. Sakthivel, S.K. Badamali, P. Selvam, Microporous Mesoporous Mater. 39 (2000) 457.
[9] S.K. Badamali, A. Sakthivel, P. Selvam, Catal. Lett. 65 (2000) 153.
[10] L.B. Young, European Patent Applied 0,029,333 (1980).
[11] R.F. Parton, J.M. Jacobs, D.R. Huybrechts, P.A. Jacobs, Stud. Surf. Sci. Catal. 46 (1988) 163.
[12] H.R. Sonawane, V.G. Naik, B.C. Subba Rao, Indian J. Chem. 3 (1965) 26.
[13] H.R. Sonawane, M.S. Wadia, B.C. Subba Rao, Indian J. Chem. 6 (1968) 72.
[14] H.R. Sonawane, M.S. Wadia, B.C. Subba Rao, Indian J. Chem. 6 (1968) 297.
[15] C. Hu, Y. Zhang, L. Xu, G. Peng, Appl. Catal. A: Gen. 177 (1999) 237.
[16] G. Sarish, B.M. Devassy, W. Böhringer, J. Fletcher, S.B. Halligudi, J. Mol. Catal. A: Chem. 240 (2005) 123.
[17] S.J. Gregg, K.S.W. Sing, Adsorption, Surface Area and Porosity, Academic Press, 1967, p. 54 (Chapter 2).